Identifying line-to-ground faulted phase in low and medium voltage AC microgrid using principal component analysis and supervised machine-learning

Muhammad Uzair*, *Member IEEE*, Li Li, *Member IEEE*, Jian Guo Zhu, *Senior Member IEEE*

***Abstract*— A supervised machine-learning based approach for faulted phase identification in bolted, low- and high-impedance line-to-ground faults using principal component analysis for feature extraction from multiple input signals is presented in this paper. DIgSILENT PowerFactory is used for simulating the underlying microgrid to obtain fault related data, while MATLAB is used for machine learning application. A 15-fold cross validation is applied to the training dataset for evaluation of different machine learning models and the results show supreme performance compared to previous methods.**

***Index Terms*— microgrid, protection, machine-learning, line-to-ground fault, principal component analysis.**

I. Introduction

With more concerns towards greenhouse gas emissions by conventional power plants in many countries including Australia and at the same time as the conventional power grid reaches its maximum capacity, more and more distributed generation (DG) sources will find their way within the modern distribution system to form a microgrid.

While microgrid brings numerous benefits, it has also caused a number of concerns, among which electrical power protection is a major challenge. For many decades, most protection schemes at the distribution level in a radial system were originally designed for one-way flow of electric power. With bidirectional power flow due to distributed generation sources, coordination between fault protection devices such as fuses, auto-recloser, overcurrent relays etc., during islanded mode can be compromised [1]. Also correct selectivity and sensitivity to avoid nuisance tripping and to avoid protection blinding such as delayed tripping or undetected faults are few of the major challenges in the practical implementation of microgrid [2]. Traditional methods will no longer provide adequate protection in future. On the other hand, application of artificial intelligence can enable learning, thinking and fast decision-making capabilities in the microgrid. Additionally, efficient and accurate single- and double-pole tripping and auto-reclosing in distribution systems will be needed for future smart grids to increase overall resilience, besides economic benefits. To achieve this, correct classification of faults and reliable faulted phase detection (or selection) are required which will also reduce system instability, avoid tripping of healthy phase or phases in an unbalanced short-circuit event or needless tripping of all three phases [3, 4].

Out of numerous faults in a three-phase system, more than 70% are line-to-ground (LG) faults [5, 6], and therefore this study focuses on detection of faulted phase in such faults. After introduction, Section II gives an overview of earlier faulted phase detection methods. Section III introduces principal component analysis (PCA) for feature extraction. System under study and the simulation results for selected cases are presented in Section IV. Section V describes in detail the proposed method for faulted phase detection followed by results and analysis in Section VI. Conclusion is given in Section VII.

II. Overview of Faulted Phase Detection Methods

Most of phase selection methods have been proposed for transmission lines, where fault parameters largely differ from distribution systems with DGs. An approach based on the current travelling waves in transmission lines is presented in [3] to classify faults and for selection of faulted-phase. This approach is ineffective for the steady state conditions [7] and is also not feasible for short-distance lines in a distribution system. Wavelet transform (WT) is used for traveling wave extraction from post-fault signals. In [8], a discrete wavelet transform (DWT) based method for identification of faulty phase in transmission lines is proposed. Haar wavelet is used for decomposition of three phases and ground current signal into approximate and detail coefficients. A threshold value is then calculated using numerical coefficient for sampling frequency and detail coefficients. Approximate coefficient of ground current is used to distinguish between line-to-line (LL) and LG faults, and then comparison of threshold value with detail coefficients separates LG from line-to-line-to-ground (LLG) faults. Similarly in [9], [4] and [10], WT is used for feature extraction from different input signals to enable fault and faulted phase detection by either identifying largest variations among three phase signals or comparing with threshold values, neither of which is suitable for implementation in microgrid as continuous changes will not

M. Uzair and Dr. L. Li are with the School of Electrical and Data Engg, University of Technology Sydney, Australia

Dr. J. Zhu is with the School of Electrical and Information Engg, The University of Sydney, Australia

Corresponding author email: uzair1@hotmail.com

allow a universal threshold value. In reference [11], fault classification method based on WT and fuzzy logic system (FLS) is proposed. DWT is used to extract energy features from current signals which are fed to FLS for classification of different fault types. This method does not identify the faulted phase. Contrary to this reference, [12] proposes a WT and FLS based phase selection algorithm using only line current signals, on the other hand reference [7] proposed an approach for selection of faulted phase based on superimposed or incremental phase voltages and currents initiated by faults, whereas [13] has proposes using superimposed negative- and positive-sequence currents to identify the faulted phase. This technique is extremely susceptible to fault resistance. In contrast, authors in [14] propose to use negative- and zero-sequence reactive power for fault classification and selection of faulted phase in single-circuit transmission lines. To determine the fault type in a microgrid, voltage angle-based and voltage angle and magnitude-based classifiers are proposed in [15]. Likewise, a fault identification and classification method for distribution systems with DGs, based on WT, is presented in [16], but the proposed method lacks identification of faulted phase.

Contrary to most researchers who have used WT, in particular DWT, for extracting features to compare them with threshold value to identify faulted phase, application of PCA to obtain predictors for machine learning (ML) classifiers is instead proposed here, as selection of the optimal mother wavelet is one of the main challenges associated with WT. Application of different mother wavelets on the signal may lead to diverse results [8, 17-19]. Moreover, DWT is largely affected by type of selected mother wavelet, giving very different results. Sampling rate and fault inception angle strongly influence DWT response as well. Consequently, most DWT based protection methods are effective for a given set of parameters and can't be generalized with the unchanged mother wavelet [20, 21]. PCA has the potential to overcome the shortcomings of WT in selection of an optimal mother wavelet basis function.

III. PCA For Feature Extraction

PCA is a powerful means for pre-processing the data before using classification or regression algorithm. It is mainly applied to reduce dimensionality and the goal is to find out latent features that actually drive the patterns instead of selecting numerous features that increases processing time. In this study, PCA identifies the composite features or principal components of the three fault signals, line-to-line voltage (*u1*), phase voltage (*u*) and short-circuit current (*Ishc*) for each phase. The fault is applied at different instances and for different spans to have a variety of data for training the ML classifier. Only first two principle components are used.

IV. Simulations

The test microgrid shown in Fig. 1 uses voltage levels from Ausgrid for Bankstown area. Three different type of loads are used, that includes a 68% dynamic industrial load connected to 11 kV Bus, unbalanced commercial load connected to Bus 3 and unbalanced residential load connected to Bus 4. The DG sources include PV unit, wind and synchronous generators.

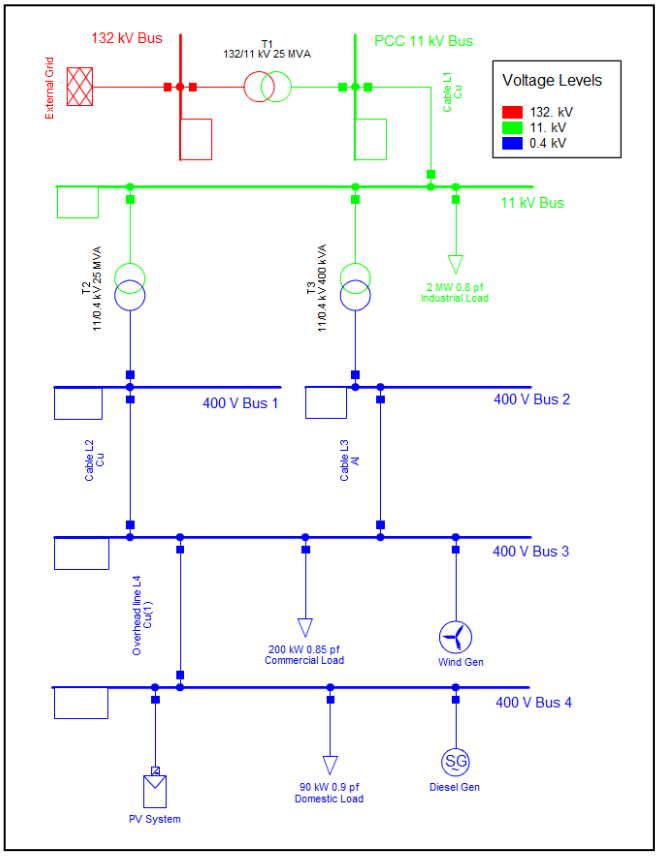

Figure 1. Test Microgrid

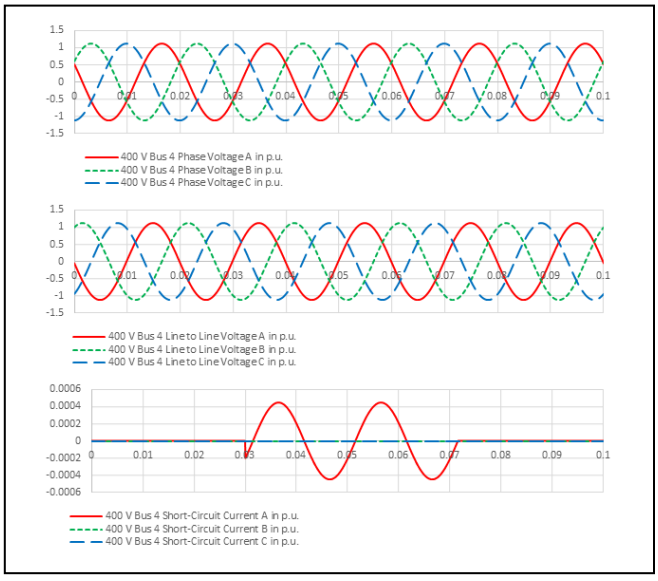

Figure 2. High impedance ground fault on phase A at 0.03 – 0.07 sec

Three different cases, high impedance ground fault (400 Ω fault resistance), bolted ground fault (0 Ω fault resistance) and low impedance ground fault (0.01 - 5 Ω fault resistance) were simulated for five different fault inception instances and durations at 11 kV, Bus 11 and 400 V Bus 4. From numerous

simulations, a few waveforms for *u*, *u1* and *Ishc* are shown below; *y*-axis is in per-unit (*pu*) and *x*-axis in *sec*.

As shown in Fig. 2, during a high impedance ground fault, there is negligible variations in line-to-line and phase voltages, and the magnitude of fault current is too low to be detected by traditional overcurrent relays. In contrast, it is visible in Fig. 3 that due to high fault current, voltage for faulted phase is zero with noticeable variations in line-to-line voltage. Fig. 4 shows variations in voltage and current waveforms for a low impedance ground fault.

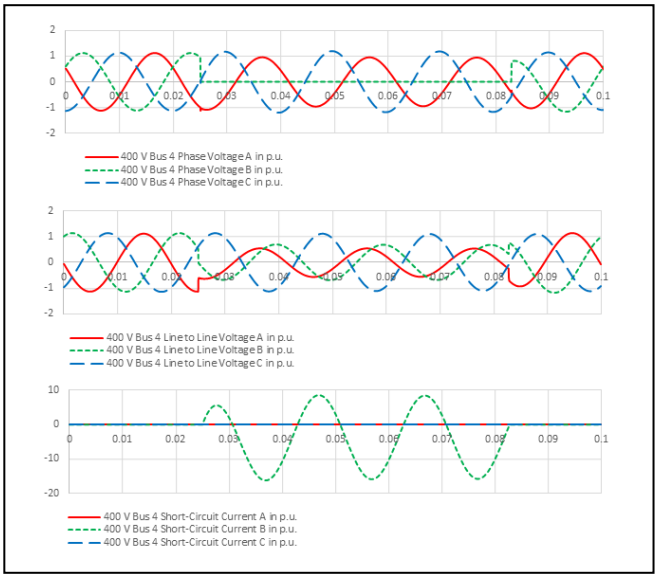

Figure 3. Bolted ground fault on phase B at 0.025 – 0.075 sec

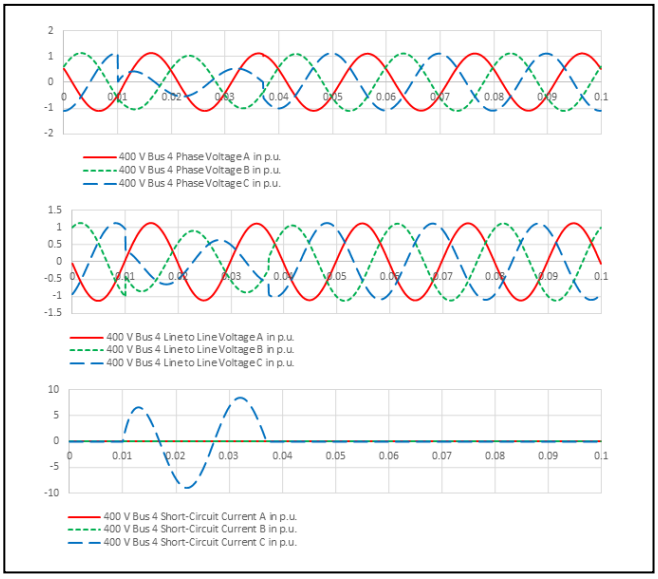

Figure 4. Low impedance ground fault on phase C at 0.01 – 0.03 sec

V. Proposed Phase-Ground Fault Detection Method

Data for 0.1 sec window is recorded through electromagnetic transient (EMT) simulations for each of the cases mentioned earlier. A step size of 0.0001 sec is used to obtain more than 1000 values for each scenario. This data is then arranged in rows and labelled for supervised ML. Using all these values for training will increase processing time and introduce overfitting, whereas manual inspection to obtain combinations that give the largest variations when the fault occurs compared to the normal operation is not possible. Moreover, using multi-dimensional data on a complex classification algorithm can result in very high variance and extremely slow processing time. To overcome these issues, application of PCA is proposed to reduce the dimensionality of input features that will optimize the performance of classification algorithm.

In this study, only the first and second principal components that capture the actual patterns in the data are used, whereas smaller principle components are ignored which just represent the noisy variations about those patterns. By choosing only the important principle components and ignoring the rest, it helps in reduction of any noise in the data. Also using only the first two principal components instead of actual values recorded, decreases the time required for classification.

The initial step in PCA is to calculate the covariance matrix for a 3-dimensional data set (*u, u*1 and *Ishc*) given by:

$$C = \begin{bmatrix} cov\,(u,u) & cov\,(u,u1) & cov\,(u,Ishc) \\ cov\,(u1,u) & cov\,(u1,u1) & cov\,(u1,Ishc) \\ cov\,(Ishc,u) & cov\,(Ishc,u1) & cov\,(Ishc,Ishc) \end{bmatrix} \tag{1}$$

where $cov\,(x,y) = \frac{\sum_{i=1}^{n}(x_i-\bar{x})(y_i-\bar{y})}{n-1}$ and $\bar{x}$ and $\bar{y}$ are the mean values of *x* and *y* respectively.

For extraction of patterns, eigenvectors are calculated for the covariance matrix based on eigenvalues given by:

$$\lambda = \begin{bmatrix} \lambda_1 & 0 & . & . & 0 \\ 0 & \lambda_2 & . & . & 0 \\ . & . & . & . & . \\ . & . & . & . & . \\ 0 & 0 & 0 & 0 & \lambda_p \end{bmatrix} \tag{2}$$

- The first eigenvector corresponds to the eigenvalue; which has the highest variance.
- The second eigenvector corresponds to the eigenvalue; which has the second highest variance.

The resulting matrix corresponds to:

$$V = [ev_1 \quad ev_2 \quad . \quad . \quad ev_p] \tag{3}$$

First and second eigenvectors are selected and remaining are ignored to obtain first and second principal components:

$$V' = [ev_1 \quad ev_2] \tag{4}$$

The new features are represented as projection of the vectors on the new base consistent to the first and second principal components.

$$pc_{1,2} = V'.[v_i - \bar{v}]^T \quad (5)$$

where $pc_{1,2}$ represents new features, whereas v_i and $\bar{v}$, represent the variable and the mean vector of original data respectively for *u, u*1 and *Ishc*.

Besides obtaining features by applying PCA, standard deviation (*std*) for *u, u*1 and *Ishc* is also used to increase the set of predictors for ML classifier training to detect faulted phase.

$$std(x) = \sqrt{\frac{\sum_{i=1}^{n}(x_i - \bar{x})^2}{(n-1)}} \quad (6)$$

The obtained various predictors are fed to three different classifiers to compare the prediction precision. These include support vector machines (SVM), K-nearest neighbors (KNN) and bagged tree (BT). An iterative process is then applied to obtain the most accurate models. After trying different kernel functions for SVM, varying number of neighbors, distance metric and weight for KNN and changing number of learners and maximum number of splits for BT, models with high accuracy are obtained. Once the models are trained, test data is applied to check the accuracy of predictions. Steps for pre-processing the data and extracting features, remains same for both training and testing. The complete process is presented in Fig. 5.

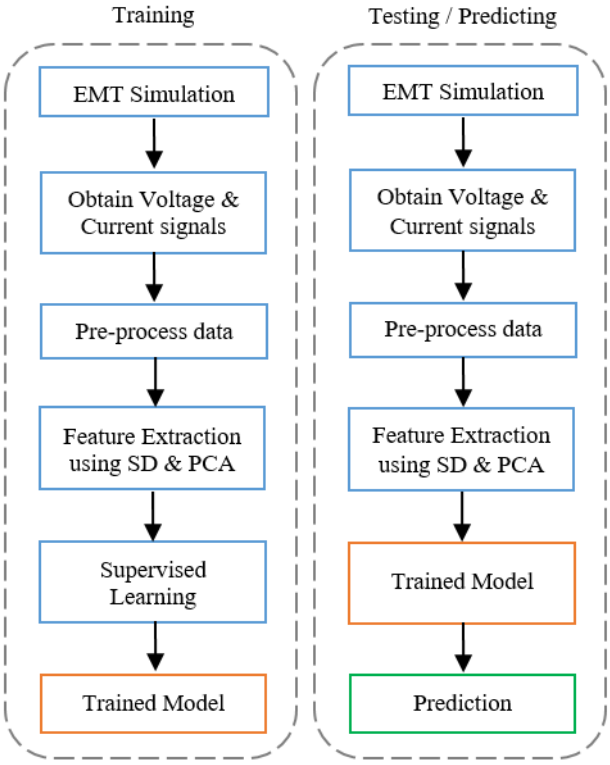

Figure 5. Proposed training and testing process of ML classifier

VI. Results and Analysis

A total of 27 predictors are obtained, including 9 for standard deviation (*std*) of 3 signals for 3 phases during fault, 9 for the first principal component (pc_1) of 3 signals for 3 phases during fault and 9 for the second principal component (pc_2) of 3 signals for 3 phases during fault. Using the 27 predictors, all the three ML classifiers accurately identified correct faulted phase, as presented in Table I.

Different combination of features (or predictors) are then used in classification model to identify and remove features with low predictive power to reduce the processing time that is vital in fault identification. It is observed that only using pc_1 with *std* predictors results in 18 predictors; and further removing predictors for *u*1 ends up with just 12 predictors; and then using *std* and pc_1 predictors for *Ishc* and pc_1 predictor for *u* also results in accurate identification. On the other hand, only using pc_1 and *std* predictors for *Ishc* slashes accuracy for SVM and BT. Alternatively only using pc_1 and removing all *std* predictors results in reduced accuracy for all three ML classifiers, while using *std* and pc_1 predictor for *u* and pc_1 predictor for *Ishc*, i.e. a combination of 9 predictors, leads to precise identification by SVM and KNN, whereas BT shows some errors.

A 15-fold cross validation has been applied to the training dataset to test the accuracy of the classifiers. Usually 5- to 10-fold cross validation is applied, but with the increase in the number of folds, variance of the resulting estimation decreases.

TABLE I. Accuracy of Identifying Correct Faulted Phase

Bolted 1Φ to ground fault at Bus 4	**ML Classifiers**		
Predictors Used	***SVM***	***KNN***	***BT***
All 27 predictors	100%	100%	100%
Different combination of 18 predictors	**100%**	**100%**	**100%**
Different combination of 12 predictors	**100%**	**100%**	**100%**
Different combination of 12 predictors	93.3%	100%	93.3%
Different combination of 9 predictors	**100%**	**100%**	**100%**
Different combination of 9 predictors	60%	86.7%	86.7%
Different combination of 9 predictors	100%	100%	93.3%

For less than 9 predictors, large inaccuracy is observed. Therefore, for further scenarios, pc_2 is not used and a combination of 9-18 predictors with highest accuracy are presented.

TABLE II. Accuracy of Identifying Correct Faulted Phase

Low Impedance Ground Fault at Bus 4	**ML Classifiers**		
Predictors Used	***SVM***	***KNN***	***BT***
All 18 predictors	100%	100%	100%
Different combination of 12 predictors	100%	100%	100%
Different combination of 9 predictors	100%	100%	100%

TABLE III. ACCURACY OF IDENTIFYING CORRECT FAULTED PHASE

High Impedance Ground Fault at Bus 4	**ML Classifiers**		
Predictors Used	***SVM***	***KNN***	***BT***
All 18 predictors	100%	100%	93.3%
Different combination of 12 predictors	100%	100%	100%
Different combination of 9 predictors	93.3%	100%	100%

TABLE IV. ACCURACY OF IDENTIFYING CORRECT FAULTED PHASE

Bolted 1Φ to ground fault at Bus 11	**ML Classifiers**		
Predictors Used	***SVM***	***KNN***	***BT***
All 18 predictors	100%	100%	100%
Different combination of 12 predictors	100%	100%	93.3%
Different combination of 9 predictors	93.3%	100%	100%

From these results, it is evident that using standard deviation and PCA for extracting predictors yields accurate identification of the faulted phase for bolted, low- and high-impedance LG faults for different fault inception instances and durations and for multiple buses in a microgrid. It is also visible that KNN shows the highest overall accuracy for various scenarios and combination of predictors for this study.

VII. CONCLUSION

This paper presented a supervised ML based approach to identify faulted phase in bolted, low- and high-impedance LG faults for various scenarios. Application of PCA for feature extraction has proven to be an excellent choice and shows that it has potential to overcome WT's shortcomings in selection of an optimal mother wavelet basis function. A 15-fold cross validation has been applied to the training dataset for evaluation of different ML models, and the results have shown supreme performance compared to previous methods. Among the three classifiers used, KNN has showed the highest overall accuracy. Future work will include classification of various faults and identification of faulted phases in LLG and LL faults which are more common after LG faults, compared to other types.

APPENDIX

27 predictors used for ML training, for high impedance case at Bus 4 are presented in following tables.

TABLE V. PREDICTORS USED FOR FAULTED PHASE IDENTIFICATION

Case: High Impedance 1Φ to ground fault at Bus 4					
pca1 u1_A	***pca2 u1_A***	***pca1 u1_B***	***pca2 u1_B***	***pca1 u1_C***	***pca2 u1_C***
0.99419	0.06255	-1.00423	-0.07167	1.01757	0.06766
0.58247	0.15379	-0.55740	-0.14402	0.57800	0.14795
0.78748	0.10790	-0.79320	-0.11543	0.77821	0.09653
-0.24332	-0.48803	0.22796	0.51272	-0.17855	-0.50669
-0.38328	-0.22677	0.42208	0.18310	-0.38919	-0.20549
-0.32202	-0.36133	0.31402	0.37909	-0.33376	-0.33048
-0.63984	0.37568	0.64174	-0.36716	-0.61756	0.30960
-0.65281	0.41791	0.66490	-0.44149	-0.64846	0.41624
-0.64939	0.40568	0.65271	-0.40314	-0.64444	0.40290
0.82527	-0.04322	-0.84701	0.02792	0.86818	-0.02160
0.43460	0.06963	-0.38776	-0.05663	0.41442	0.06508
0.62540	0.01088	-0.63867	-0.02247	0.59522	0.00075
-0.44369	-0.20511	0.40919	0.25435	-0.44015	-0.26941
-0.43196	-0.18719	0.44212	0.13662	-0.47420	-0.14901
-0.48309	-0.09238	0.45355	0.12823	-0.52527	-0.02403

TABLE VI. PREDICTORS USED FOR FAULTED PHASE IDENTIFICATION

Case: High Impedance 1Φ to ground fault at Bus 4					
pca1 u_A	***pca2 u_A***	***pca1 u_B***	***pca2 u_B***	***pca1 u_C***	***pca2 u_C***
1.00650	-0.06281	-0.99298	-0.06741	1.01652	0.07159
0.58775	-0.15316	-0.56723	-0.14944	0.56289	0.14319
0.77939	-0.09790	-0.79429	-0.11677	0.78520	0.10521
-0.20510	0.49223	0.25447	0.49910	-0.19023	-0.51627
-0.37446	0.22812	0.40695	0.20408	-0.41313	-0.18322
-0.33251	0.33484	0.31291	0.38253	-0.32439	-0.35353
-0.62426	-0.33523	0.64886	-0.39057	-0.62603	0.32661
-0.64616	-0.40840	0.66205	-0.43365	-0.65796	0.43365
-0.64501	-0.40406	0.65355	-0.40547	-0.64798	0.40212
0.84677	0.03418	-0.82545	0.03980	0.86827	-0.01883
0.43657	-0.07100	-0.41021	-0.06277	0.38999	0.05763
0.60084	-0.00078	-0.64436	-0.02157	0.61409	0.01182
-0.45248	0.23050	0.42196	0.21896	-0.41860	-0.27942
-0.45685	0.17942	0.42446	0.16514	-0.46698	-0.12825
-0.52099	0.03406	0.44929	0.13805	-0.49165	-0.07231

TABLE VII. PREDICTORS USED FOR FAULTED PHASE IDENTIFICATION

Case: High Impedance 1Φ to ground fault at Bus 4					
pca1 Ishc_A	***pca2 Ishc _A***	***pca1 Ishc _B***	***pca2 Ishc_B***	***pca1 Ishc _A***	***pca2 Ishc _C***
-0.00065	0.00334	0.00188	0.00047	0.00178	0.00055
-0.00165	-0.00057	-0.00051	-0.00416	0.00178	0.00055
-0.00165	-0.00057	0.00188	0.00047	0.00016	-0.00380
0.00396	-0.00180	0.00188	0.00047	0.00178	0.00055
-0.00165	-0.00057	-0.00476	0.00194	0.00178	0.00055
-0.00165	-0.00057	0.00188	0.00047	-0.00426	0.00166
0.00649	-0.00013	0.00188	0.00047	0.00178	0.00055
-0.00165	-0.00057	-0.00657	0.00036	0.00178	0.00055
-0.00165	-0.00057	0.00188	0.00047	-0.00660	0.00028
0.00085	0.00482	0.00188	0.00047	0.00178	0.00055
-0.00165	-0.00057	-0.00196	-0.00449	0.00178	0.00055
-0.00165	-0.00057	0.00188	0.00047	-0.00132	-0.00476
0.00581	-0.00057	0.00188	0.00047	0.00178	0.00055
-0.00165	-0.00057	-0.00500	0.00164	0.00178	0.00055
-0.00165	-0.00057	0.00188	0.00047	-0.00578	0.00112

TABLE VIII. PREDICTORS USED FOR FAULTED PHASE IDENTIFICATION

Case: High Impedance 1Φ to ground fault at Bus 4					
std u1_A	***std u1_B***	***std u1_C***	***std u_A***	***std u_B***	***std u_C***
0.79480	0.79724	0.79601	0.79479	0.79603	0.79723
0.79466	0.79647	0.79693	0.79557	0.79511	0.79738

0.79560	0.79632	0.79614	0.79573	0.79590	0.79644
0.79480	0.79724	0.79601	0.79479	0.79603	0.79723
0.79466	0.79647	0.79693	0.79557	0.79511	0.79738
0.79560	0.79632	0.79614	0.79573	0.79590	0.79644
0.79480	0.79725	0.79601	0.79479	0.79603	0.79724
0.79466	0.79646	0.79693	0.79557	0.79511	0.79738
0.79560	0.79632	0.79613	0.79572	0.79590	0.79643
0.79545	0.79685	0.79575	0.79518	0.79628	0.79658
0.79531	0.79607	0.79668	0.79596	0.79536	0.79673
0.79625	0.79592	0.79588	0.79612	0.79615	0.79579
0.79623	0.79639	0.79544	0.79565	0.79660	0.79580
0.79610	0.79560	0.79636	0.79643	0.79568	0.79594
0.79704	0.79546	0.79557	0.79659	0.79647	0.79500

TABLE IX. PREDICTORS USED FOR FAULTED PHASE IDENTIFICATION

std Ishc_A	***std Ishc _B***	***std Ishc _C***
0.00014	0.00000	0.00000
0.00000	0.00017	0.00000
0.00000	0.00000	0.00016
0.00020	0.00000	0.00000
0.00000	0.00022	0.00000
0.00000	0.00000	0.00021
0.00026	0.00000	0.00000
0.00000	0.00028	0.00000
0.00000	0.00000	0.00027
0.00020	0.00000	0.00000
0.00000	0.00021	0.00000
0.00000	0.00000	0.00020
0.00024	0.00000	0.00000
0.00000	0.00023	0.00000
0.00000	0.00000	0.00025

REFERENCES

[1] L. Fusheng, L. Ruisheng, and Z. Fengquan, "Chapter 5 - Protection of the microgrid," in *Microgrid Technology and Engineering Application*Oxford: Academic Press, 2016, pp. 69-89.

[2] M. R. Islam and H. A. Gabbar, "Analysis of Microgrid protection strategies," in *2012 International Conference on Smart Grid (SGE)*, 2012, pp. 1-6.

[3] X. Dong, W. Kong, and T. Cui, "Fault Classification and Faulted-Phase Selection Based on the Initial Current Traveling Wave," *IEEE Transactions on Power Delivery,* vol. 24, no. 2, pp. 552-559, 2009.

[4] O. A. S. Youssef, "New algorithm to phase selection based on wavelet transforms," *IEEE Transactions on Power Delivery,* vol. 17, no. 4, pp. 908-914, 2002.

[5] M. F. McGranaghan, D. R. Mueller, and M. J. Samotyj, "Voltage sags in industrial systems," *IEEE Transactions on Industry Applications,* vol. 29, no. 2, pp. 397-403, 1993.

[6] B. Brown. (05 Aug). *System Grounding*. Available: http://static.schneider-electric.us/assets/consultingengineer/appguidedocs/section6_0307.pdf

[7] D. W. P. Thomas, M. S. Jones, and C. Christopoulos, "Phase selection based on superimposed components," *IEE Proceedings - Generation, Transmission and Distribution,* vol. 143, no. 3, pp. 295-299, 1996.

[8] M. I. Zaki, R. A. E. Sehiemy, G. M. Amer, and F. M. A. E. Enin, "Integrated discrete wavelet transform-based faulted phase identification for multi-terminals power systems," in *2017 Nineteenth International Middle East Power Systems Conference (MEPCON)*, 2017, pp. 503-509.

[9] C. Aguilera, E. Orduna, and G. Ratta, "Fault detection, classification and faulted phase selection approach based on high-frequency voltage signals applied to a series-compensated line," *IEE Proceedings - Generation, Transmission and Distribution,* vol. 153, no. 4, pp. 469-475, 2006.

[10] J. Joe-Air, F. Ping-Lin, C. Ching-Shan, Y. Chi-Shan, and S. Jin-Yi, "A fault detection and faulted-phase selection approach for transmission lines with Haar wavelet transform," in *2003 IEEE PES Transmission and Distribution Conference and Exposition (IEEE Cat. No.03CH37495)*, 2003, vol. 1, pp. 285-289 Vol.1.

[11] M. Jamil, R. Singh, and S. K. Sharma, "Fault identification in electrical power distribution system using combined discrete wavelet transform and fuzzy logic," *Journal of Electrical Systems and Information Technology,* vol. 2, no. 2, pp. 257-267, 2015/09/01/ 2015.

[12] O. A. S. Youssef, "A novel fuzzy-logic-based phase selection technique for power system relaying," *Electric Power Systems Research,* vol. 68, no. 3, pp. 175-184, 2004/03/01/ 2004.

[13] L. Xiang-Ning, Z. Menghua, K. Alymann, and L. Pei, "Novel design of a fast phase selector using correlation analysis," *IEEE Transactions on Power Delivery,* vol. 20, no. 2, pp. 1283-1290, 2005.

[14] B. Mahamedi and J. G. Zhu, "Fault Classification and Faulted Phase Selection Based on the Symmetrical Components of Reactive Power for Single-Circuit Transmission Lines," *IEEE Transactions on Power Delivery,* vol. 28, no. 4, pp. 2326-2332, 2013.

[15] A. Hooshyar, E. F. El-Saadany, and M. Sanaye-Pasand, "Fault Type Classification in Microgrids Including Photovoltaic DGs," *IEEE Transactions on Smart Grid,* vol. 7, no. 5, pp. 2218-2229, 2016.

[16] A. C. Adewole and R. Tzoneva, "Fault detection and classification in a distribution network integrated with distributed generators," in *IEEE Power and Energy Society Conference and Exposition in Africa: Intelligent Grid Integration of Renewable Energy Resources (PowerAfrica)*, 2012, pp. 1-8.

[17] F. B. Costa, A. H. P. Sobrinho, M. Ansaldi, and M. A. D. Almeida, "The effects of the mother wavelet for transmission line fault detection and classification," in *Proceedings of the 2011 3rd International Youth Conference on Energetics (IYCE)*, 2011, pp. 1-6.

[18] W. K. Ngui, M. S. Leong, L. M. Hee, and A. M. Abdelrhman, "Wavelet Analysis: Mother Wavelet Selection Methods," *Applied Mechanics and Materials,* vol. 393, pp. 953-958, 2013.

[19] W. A. Wilkinson and M. D. Cox, "Discrete wavelet analysis of power system transients," *IEEE Transactions on Power Systems,* vol. 11, no. 4, pp. 2038-2044, 1996.

[20] H. A. Darwish, M. Hesham, A. I. Taalab, and N. M. Mansour, "Close Accord on DWT Performance and Real-Time Implementation for Protection Applications," *IEEE Transactions on Power Delivery,* vol. 25, no. 4, pp. 2174-2183, 2010.

[21] H. A. Darwish, A. I. Taalab, A. H. Osman, N. M. Mansour, and O. P. Malik, "Spectral Energy Differential Approach for Transmission Line Protection," in *2006 IEEE PES Power Systems Conference and Exposition*, 2006, pp. 1931-1937.